AGU PUBLICATIONS

Tectonics

RESEARCH ARTICLE
10.1002/2015TC004057

Key Points:
- We performed an integrative analysis of geological gravimetric and seismological data
- Analyzed data depicted a not well-known wrench zone in the central-eastern Sicily
- Our findings enabled us to interpret this shear zone as a Plio-Pleistocene STEP fault

Correspondence to:
G. Barreca,
g.barreca@unict.it

Citation:
Barreca, G., L. Scarfì, F. Cannavò, I. Koulakov, and C. Monaco (2016), New structural and seismological evidence and interpretation of a lithospheric-scale shear zone at the southern edge of the Ionian subduction system (central-eastern Sicily, Italy), *Tectonics*, *35*, 1489–1505, doi:10.1002/2015TC004057.

Received 14 OCT 2015
Accepted 30 MAY 2016
Accepted article online 4 JUN 2016
Published online 22 JUN 2016

New structural and seismological evidence and interpretation of a lithospheric-scale shear zone at the southern edge of the Ionian subduction system (central-eastern Sicily, Italy)

G. Barreca[1], L. Scarfì[2], F. Cannavò[2], I. Koulakov[3], and C. Monaco[1]

[1]Dipartimento di Scienze Biologiche, Geologiche e Ambientali, Università di Catania, Sezione di Scienze della Terra, Catania, Italy, [2]Istituto Nazionale di Geofisica e Vulcanologia, Osservatorio Etneo, Catania, Italy, [3]Institute of Petroleum Geology and Geophysics, Novosibirsk, Russia

Abstract Geological, gravimetric, and seismological data from the central-eastern Sicily (Italy) provide evidences of a NW-SE oriented shear zone at the southern edge of the Ionian subduction system. This structure consists of a near 100 km long lithospheric-scale structural and seismic boundary. In the near-surface, it shows Plio-Pleistocene vertical-axis structural rotations, kilometer-scale topographic imprint, progressive wrenching, and large down-faulting. All these features, together with its location south-west of the subduction system, allow us to interpret the shear zone as the upper plate expression of an abandoned Subduction Transform Edge Propagator fault, working before slab detachment, currently reactivated by elastic rebound or mantle upwelling mechanism triggered by slab detachment, to form an incipient transform belt separating compartments characterized by different motion in the modern context of Africa-Europe convergence.

1. Introduction

As documented by abundant literature, the Sicilian Collision Zone in southern Italy (Figure 1) has a long tectonic history that produced multideformed rock units. In particular, many investigators in the past decades [e.g., *Ghisetti and Vezzani*, 1982; *Finetti et al.*, 1996, 2005; *Barreca et al.*, 2010a, 2010b; *Barreca and Maesano*, 2012] have pointed out the role of wrench tectonics in the Plio-Quaternary geodynamics of the Sicilian Collision Zone at the transition to the Ionian-Calabrian subduction system, including the Tyrrhenian offshore. Although different interpretations on mode, role, and timing still remain, the development of shear zones along the Sicilian Chain conforms well with the oblique Africa-Eurasia convergence dynamics [*Dewey et al.*, 1989].

A critical reading of previously published regional-scale geological/structural maps [e.g., *Finetti et al.*, 2005, and others minor maps] highlights that the trends of the main structural features of the Sicilian Collision Zone significantly change (from NE-SW to NW-SE) along a preferential zone extending roughly from the central-northern Sicily as far as the SW of Mount Etna (Figure 1c). Taking into account that vertical-axis structural rotations can develop only during thrust sheet piling or lateral wrenching and that tearing is expected along continental Sicily according to the shifting of the Calabrian Arc toward the SE (Figure 1a), the strong variation in the structural trends could be produced by large-scale wrench tectonics. Systematic clockwise versus of rotations of major basins and thrusts along this area are consistent with the occurrence of a regional-scale shear zone. To better constrain this supposed mechanism of deformation, a multiscale analysis of geological, gravimetric, and seismological data has been performed. The examined data all point to the occurrence of a NW-SE oriented dextral wrench zone slicing through right across the central-eastern portion of the Sicilian fold and thrust belt, between the Madonie Mountains and Mount Judica area (Figure 1c). In addition, previous seismologic [*Neri et al.*, 2005], geodetic [*Devoti et al.*, 2011; *Palano et al.*, 2012], and geological [*Billi et al.*, 2010] data highlighted the occurrence of an extensional belt affecting the same area. Although *Lavecchia et al.* [2007] viewed this incipient extension as ensuing from upper crustal stretching above an active thrust belt, *Billi et al.* [2010] favored reactivation of preexisting faults, favorably oriented with respect to the convergence direction, and upwelling of melt mantle material beneath Mount Etna.

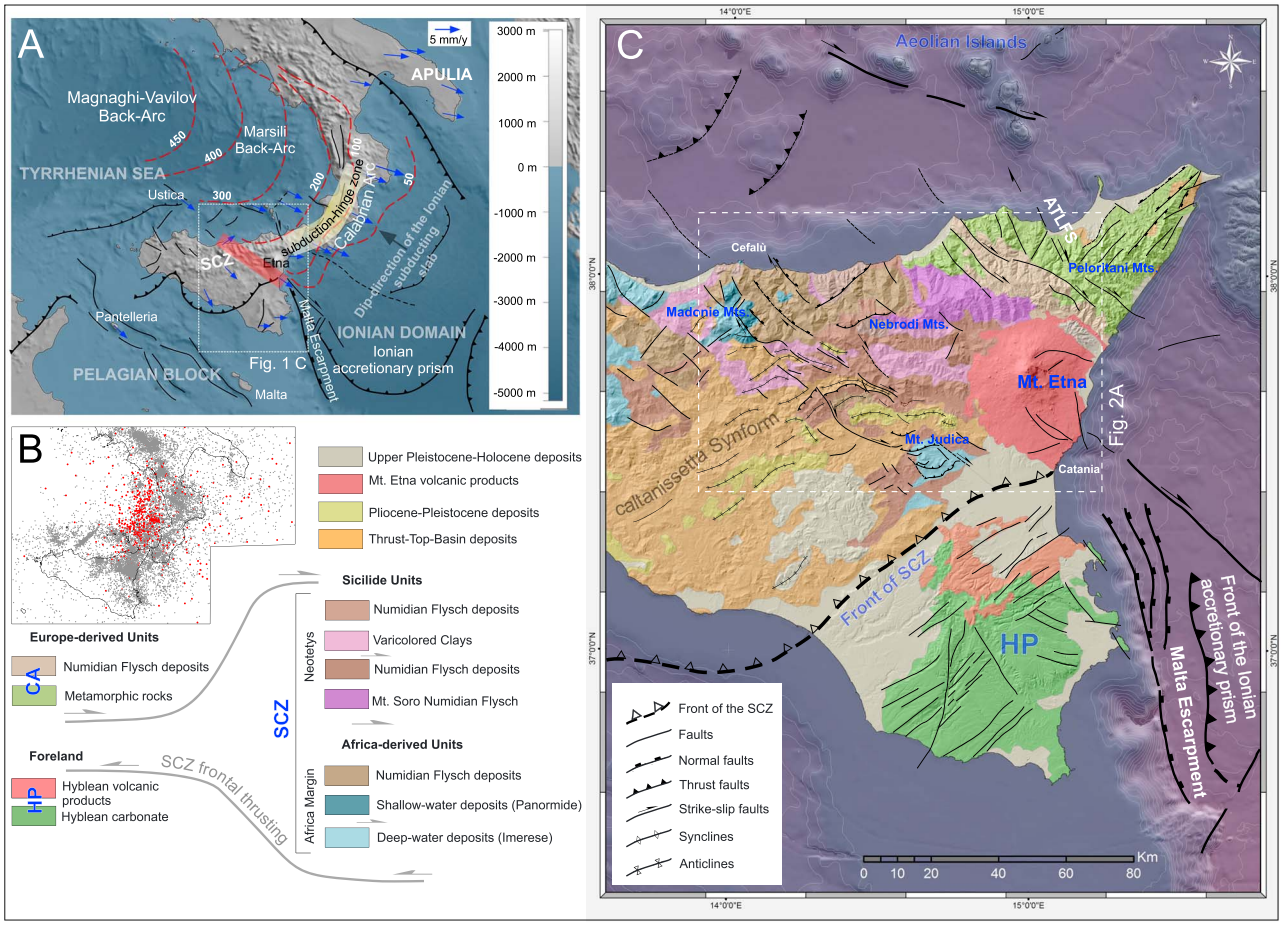

Figure 1. (a) Shaded-relief map of the Central Mediterranean showing the major tectonic features. The red dashed lines represent the Benioff-Wadati contours depicting the NW-ward descending Ionian slab [from *Sartori*, 2003]. The blue arrows indicate the current horizontal GPS velocity field [from *Mastrolembo Ventura et al.*, 2014] in the Nubia reference frame. The transparent red rectangle is the analyzed region at the SW edge of the Ionian/Calabrian subduction system, and the light-yellow box represents the present-day slab zone [from *Neri et al.*, 2009]. (b) Seismicity of central Mediterranean over the last 20 years (http://csi.rm.ingv.it/; http://bollettinosismico.rm.ingv.it/index.php); the red dots indicate very deep earthquakes related to the active part of the Ionian slab. (c) Structural sketch map of central-eastern Sicily [after *Finetti et al.*, 2005] showing the general tectonic setting of this region; offshore faults are from *Polonia et al.* [2011] and *Gutscher et al.* [2015]. Bathymetry data from SRTM 30 plus (Shuttle Radar Tomography Mission http://topex.ucsd.edu/WWW_html/srtm30_plus.html).

New geological and seismological studies have enabled us to better define the architecture and kinematic evolution of this complex first-order structural/seismic belt, located about 100 km far from the southwestern edge of the Ionian-Calabrian subduction system, and to suggest its possible role in the wider context of collisional/subduction dynamics of the central Mediterranean.

2. Geodynamic Framework

2.1. Tectonic Background

In the central Mediterranean, several crustal compartments of a former paleogeographic configuration have been involved in the long-living convergence between African and Eurasian plates [*Malinverno and Ryan*, 1986; *Dewey et al.*, 1989; *Jolivet and Faccenna*, 2000; *Ben Avraham et al.*, 1990]. In this scenario, mobile blocks with different thickness and rheology (e.g., continental or oceanic) support the setting of a collisional/subduction zone with associated accretionary wedges and the development of an intricate back-arc/fore-arc/trench system [*Scandone*, 1979; *Malinverno and Ryan*, 1986; *Patacca and Scandone*, 1989; *Faccenna et al.*, 2004]. This latter include the Tyrrhenian stretched area, the Ionian subduction complex, and the orogenic domain, represented by the Calabrian Arc (CA), the subaerial part of a larger accretionary

prism in the Ionian Sea (Figure 1a), which is bounded, to the southwest, by the Sicilian Collision Zone (SCZ). The back-arc system occupies the southern portion of the Tyrrhenian Sea and consists of a series of basins, settled in a thinned crustal domain, that host volcanic seamounts (e.g., the Magnaghi-Vavilov and Marsili; see Figure 1a). These basins opened since the early Pliocene [*Kastens et al.*, 1988] in response to stretching related to the progressive retreating of the Ionian slab toward the SE. The Ionian realm, a 15–20 km thick crustal remnant [*Catalano et al.*, 2001; *Vai*, 2003] of a Permo-Triassic ocean (the Neo-Tethys [*Şengör*, 1979]), is adjacent to a Tertiary-Quaternary foreland domain, the Pelagian Block [*Ben-Avraham and Grasso*, 1991] (Figure 1a), which also includes the 25–30 km thick continental crustal portion of the Hyblean Plateau in SE Sicily (HP in Figure 1c). The transition (continental to oceanic) between these two distinct lithospheric compartments is inferred to occur in the near offshore of eastern Sicily along the Malta Escarpment, a Mesozoic passive margin which has been reactivated by oblique extension during Plio-Quaternary times [*Fabbri et al.*, 1982; *Casero et al.*, 1984].

As suggested by the intermediate and deep seismicity (up to 600 km [*Frepoli et al.*, 1996]), the Ionian crust descends beneath the Calabrian Arc where it forms a narrow subduction zone with an ~70°NW dipping Benioff-Wadati zone (see the dashed red lines in Figure 1a). Tomographic models [e.g.,*Wortel and Spakman*, 2000; *Calò et al.*, 2009; *Neri et al.*, 2009] show that the subducting slab is in-depth continuous only in Southern Calabria, whereas the lack of deep seismicity in Sicily and southern Apennines (Figure 1b) suggests slab tear deformation at the NE and SW edges of this subduction zone [*Orecchio et al.*, 2014].

The SCZ, west of the Ionian subduction (see Figure 1a), originated from the deformation of the Africa continental paleo-margin (the northern margin of the Pelagian Block) [*Bianchi et al.*, 1987; *Roure et al.*, 1990; *Bello et al.*, 2000] and of the Neo-Tethys oceanic realm [*Şengör*, 1979], located between the European Block to the North and the Pelagian Block to the South.

Convergence has involved these sectors since the Neogene, giving rise to a wide collision zone (SCZ, in Figure 1a), a SE-verging contractional belt formed by imbricate stacks of Meso-Cenozoic shallow to deep-water carbonate series and oceanic units. Africa margin-derived units mostly outcrop in the central-western portion of the SCZ, whereas the oceanic units are sandwiched along a NW-SE oriented belt in north-eastern Sicily. Toward the NE, the oceanic units are confined by an important tectonic boundary (e.g., the Taormina Line [see *Ghisetti and Vezzani*, 1982]), which separates the Sicilian-Maghrebian belt from the Calabrian terranes.

Thrust migration in the SCZ was accompanied by sedimentation in piggyback basins [*Grasso and Butler*, 1991; *Barreca*, 2014a], mostly preserved in the south-western portion of the collision zone (Figure 1c). Deep thrusting is still active along the SCZ [*Lavecchia et al.*, 2007] as testified by the occurrence of destructive earthquakes in historical and recent times [*Monaco et al.*, 1996; *Guidoboni et al.*, 2002; *Barreca et al.*, 2014a]

Accordingly, the occurrence at the same time of ongoing collision and subduction with uneven tectonic rates, higher in the unconstrained CA, lower in the almost-locked SCZ, has resulted since Pliocene times in the development of a transfer zone at the transition between these two kinematic domains. This gave rise in the north-eastern border of the SCZ to a widespread ~NW-SE trending dextral wrenching faults system (see also the Southern Tyrrhenian System of *Finetti et al.* [1996]). At a more detailed scale, this wrenching zone is characterized by scattered and en-echelon arranged fault segments, which sometimes give rise to restraining/releasing zones in the overlapping sectors [*Barreca et al.*, 2010a; *Barreca and Maesano*, 2012]. In many cases the shearing is accompanied by structural rotations of previously settled tectonic features [*Barreca and Monaco*, 2013; *Barreca*, 2014a, and reference therein]. This structural setting, dominated by wrenching deformation, still reflects in the present-day distribution of crustal and shallow seismicity, of which focal mechanisms are mostly characterized by strike-slip, normal, and reverse-oblique kinematics that are compatible with low-dip NNW-SSE to NNE-SSW trending *P* axes [*Neri et al.*, 2005].

2.2. Current Kinematics of the Sicilian-Calabrian Collision/Subduction System

Compared to the rates of propagation, which are recorded in other subduction/trench systems throughout the world (i.e., 9 mm in Gibraltar, 18 mm in Lesser Antilles, and 158 mm/yr in Tonga [see *Schellart et al.*, 2007]), the Calabrian Arc currently migrates at a very low rate (~2 mm/yr [*D'Agostino et al.*, 2011]). This velocity implies a strong deceleration with respect to the migration rate at 6–8 cm/yr of the Calabrian trench in the

last 8–10 Ma (until the middle Pleistocene [*Goes et al.*, 2004; *Billi et al.*, 2011]), when the subduction process of the Ionian slab was substantially controlled by rapid slab roll-back and fast back-arc extension [*Faccenna et al.*, 2001]. Considering the progressive narrowing of the Calabrian Arc, this deceleration is in contrast with the numerical models by *Schellart et al.* [2007], predicting that narrow subduction zones roll-back at much higher rates than wider zones, due to the toroidal component of the flow field, influencing the whole slab surface. This apparent inconsistency can be related to the near-cessation of the Calabrian roll-back and stalling of the slab subduction [*Faccenna et al.*, 2001; *Goes et al.*, 2004] with consequent readjustment of plate boundaries, which has affected the central Mediterranean arc/trench migration since the Middle Pleistocene (0.8–0.5 Ma).

Plate reorganization mechanism is suggested by current GPS velocities [*Palano et al.*, 2012, and reference therein] and available fault plane solutions [*Neri et al.*, 2005; *Pondrelli et al.*, 2004, 2006; *Presti et al.*, 2013; *Scarfì et al.*, 2013], which display a fragmentation of the south-eastern Mediterranean into crustal blocks with independent kinematics separated by seismically active belts [*Palano et al.*, 2012; *Mastrolembo Ventura et al.*, 2014] that locally form triple junction at their boundaries [*Barreca et al.*, 2014b]. In this framework, the never-ceased convergence between Africa and Eurasian Plates has renewed, and to date, it seems to prevail over back-arc extension dynamics in the southern Tyrrhenian Sea, at the rear of the SCZ, with the formation of a compressive belt juxtaposed to the extensional belt, still active in NE Sicily and western Calabria, by a transversal NNW-SSE oriented tectonic boundary, the Aeolian-Tindari-Letojanni fault system (ATLFS in Figure 1b [*Billi et al.*, 2006, 2011; *Pondrelli et al.*, 2004, 2006; *Palano et al.*, 2012]).

3. New Data

3.1. Methods

Investigation in the study area has been performed using an extensive data set that includes both original and large-scale geological/geophysical data available from the literature. Original data consist of detailed field measurements (i.e., kinematic indicators along major fault planes and fold axis trends) and seismological data and tools aimed at structurally constraining the shallow portion of the zone extending from the central-northern Sicily as far as the SW of Mount Etna and to define its deep architecture and current activity/kinematics. Field data were mainly collected along the central and northern sector of the belt, while its south-eastern tip has been structurally constrained by using data coming from a previous work of one of the authors [*Monaco and De Guidi*, 2006]. Commercial boreholes, stored into available Web digital databases (the Vi.De.Pi. Project, http://unmig.sviluppoeconomico.gov.it), provided clues to determine the magnitude of vertical and lateral displacement for the fault zone.

Seismic input was obtained by local seismicity routinely recorded by the Istituto Nazionale di Geofisica e Vulcanologia since the 1980s. In particular, seismic parameters (i.e., *P* and *S* wave observations) were inverted to obtain a 3-D velocity structure and the hypocentral locations over the central-eastern Sicily. Moreover, computed fault plane solutions were used to describe the crustal faulting regime.

Further, information about the possible paleo-tectonic framework of the area have been achieved by the tectonic interpretation of a recently published gravimetric gradient map of the central Mediterranean [*Barreca*, 2014b]. This consists of a slope representation of Bouguer gravity anomalies and provides a rapid and bi-dimensional view of lateral changes of Bouguer trends (i.e., where high-density rocks and soft sediments are juxtaposed, e.g., along faults or paleo-margins), not usually identifiable using traditional equipotential contours maps (see *Barreca* [2014b] for further information).

In the following paragraphs, we give details on the analyses carried out on geological, gravimetric, and seismological data.

3.2. Field Data

Field/structural analysis were carried out in central-eastern Sicily between the Madonie Mountain range and the Mount Judica area (SW of Mount Etna volcano) (Figure 2a) in order to kinematically constrain the regional-scale belt. To the North, the Madonie Mountain range, on the western side of the wrench zone (see Figures 1b and 2a for location), is a structural/topographic culmination (~2000 m above sea level (asl)) of the SCZ, formed by a Miocene thrust-stack of shallow and deepwater Meso-Cenozoic carbonate successions belonging to the African paleo-margin, locally known as Panormide units and Imerese units,

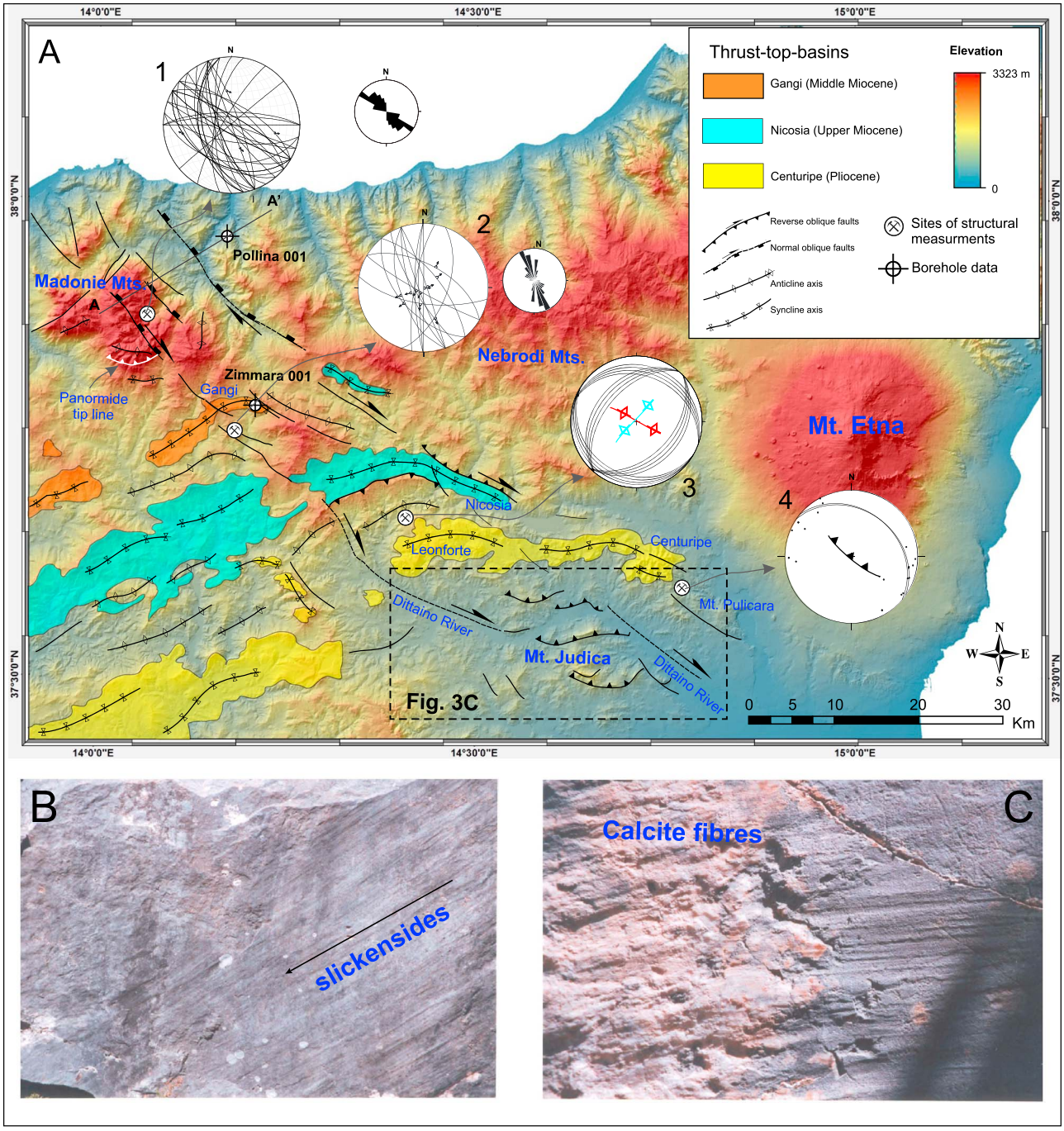

Figure 2. (a) Altitude/shaded relief map of central eastern Sicily highlighting the major Mio-Pliocene Thrust-top basins and the fault segments making up the shear zone between the Madonie Mountains in the NW and Mount Judica in the SE. Note the hock-shape geometry of the three basins (Gangi, Nicosia, and Centuripe) at their NE termination. This configuration has been interpreted as related to clockwise, vertical-axis structural rotations produced by the right-lateral motion of the bounding wrench fault. (b) Motion has been constrained by structural analysis at key points (see plots in Figure 2a) by measuring kinematic indicators, e.g., (c) slickensides and calcite fibres.

respectively [*Grasso et al.*, 1978, and reference therein]. The Panormide unit mainly outcrops in the eastern part of the Madonie Mountain Range, where it occupies the highest structural position forming a NNW-SSE oriented carbonate plateau (Figure 1c), which extends southwards as far as its tip line (Figure 2a). East of the wrench zone, the Panormide carbonates sharply disappear and their Miocene terrigenous covers outcrop

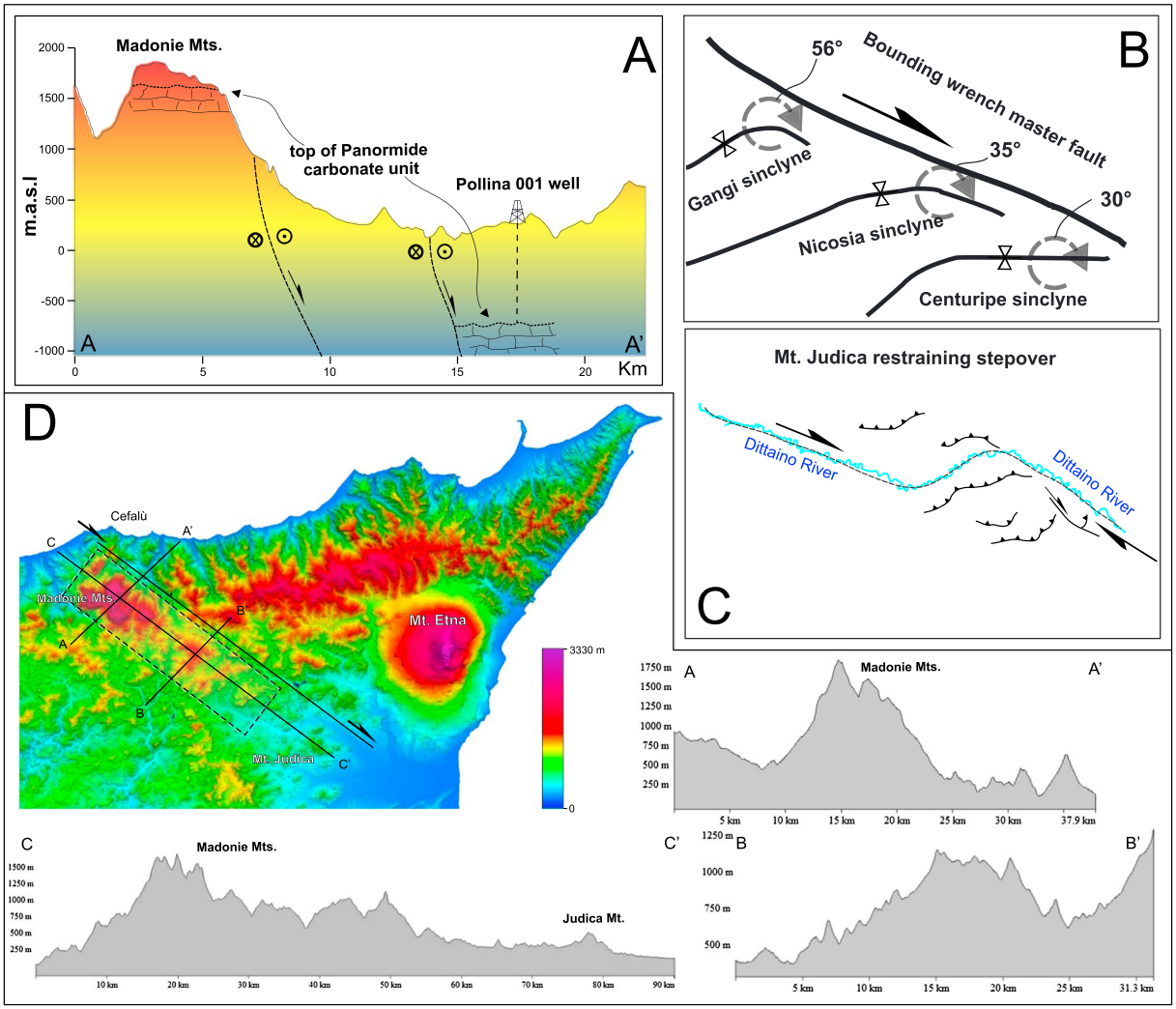

Figure 3. (a) Reconstructed geological section across the NW segment of the wrench zone (see Figure 2a for location) showing extreme down-faulting in the area. (b) The central sector of the faulted zone displays systematic clockwise rotations, whose degree suggests progressive wrenching of the fault. (c) SE-ward, between the Centuripe basin and Mount Judica, the wrench zone became wider and shows en-echelon segments that give rise to the Mount Judica restraining step over. (d) DTM of central-eastern Sicily showing the topographic setting in the vicinity of the faulted zone. Altitude profiles revealed a kilometer-scale NW-SE elongated topographic high in the SW side of the faulted zone.

about 1500 m further downslope. Structural measurements performed along the transition between the two sectors lying at different altitudes (see Figure 2a for location) revealed that this zone is deformed by a NW-SE oriented fault array. Collected mesofaults (~60 plane, see plot no. 1 in Figure 2a) mainly dip toward the east and some of them show striated planes (Figure 2b) and calcite fibres (Figure 2c) indicating pure to normal-oblique (right-lateral) motion.

A log provided by the commercial Pollina 001 well (Vi.De.Pi. Project, http://unmig.sviluppoeconomico.gov.it/deposito/pozzi/log/pdf/pollina_001.pdf; see Figure 2a for location) shows that the top of the Panormide carbonates has been drilled at ~700 m below sea level, accounting for a down-faulting of about 2.7 km, since it outcrops at about 2000 m asl along the Madonie Mountains (Figure 3a). Age of deformation can be referred to the post-Pliocene times as testified by diffused normal faults cross-cutting the Pliocene [*Abate et al.*, 1982] thrusts along the Madonie Mountain range [*ISPRA,* 2012]. Widespread faulting also occurs SE-ward, in the nearby of the Gangi village.

Measured planes (~20) and kinematic indicators evidenced a NNW-SSE trending normal to oblique fault belt (see plot 2 in Figure 2a), transversally cutting the Gangi syncline. At the core of the Gangi syncline, another

log (the Zimmara 001 well, Vi.De.Pi. Project http://unmig.sviluppoeconomico.gov.it/deposito/pozzi/log/pdf/zimmara_001.pdf; see Figure 2a for location) shows that the Panormide carbonates have drilled again at a depth of ~2100 m. Considering that the well is located about 20 km southeast from the outcropping Panormide tip line (see Figure 2a for location), a lateral displacement of at least the same amount can be estimated for this segment of the wrench zone.

Along the central sector of the wrench zone, clockwise rotations of the major NE-SW trending Mio-Pliocene compressive structures of the SCZ are observed. This process involved three regional-scale Neogene satellite basins of the SCZ, whose deposits are preserved in synforms located in the SW side of the wrench fault system (the Gangi, Nicosia, and Centuripe synclines; Figure 2a). These structures have been systematically dragged/rotated around the vertical axis and have assumed a hook-shape at their NE terminations becoming roughly coaxial to the bounding wrench zone (Figure 2a). The amount of rotation decreases from NW to SE (56° in the Gangi syncline, 35° in the Nicosia syncline, and 30° in the Centuripe syncline; Figure 3b). Structural measurement performed on folded gypsum layers north of the Leonforte Village, between the Centuripe and Nicosia synclines (see Figure 2a for location), evidenced the occurrence of two folding phases, which have produced mesoscale interference pattern (dome and basin structures) characterized by folds with nearly-orthogonal axes trending NE-SW and NW-SE, respectively (see plot 3 in Figure 2a).Wrench-related vertical axis rotations are also corroborated by the presence of rotated WNW-ESE trending thrusts and folds involving early Pliocene sediments near Mount Pulicara locality, to the east (see *Monaco and De Guidi* [2006] and plot 4 in Figure 2a).

The south-eastern sector of the wrench zone (Mount Judica area; see Figure 2a for location) is characterized by the occurrence of discrete segments of right-lateral strike-slip faults, roughly distributed within a 15–20 km wide deformation zone. The ridges forming the Mount Judica thrust system (involving the deep-water Imerese unit; see Figure 2a), nucleated within a restraining step over formed at the left-stepping zone of major dextral strike-slip fault segments (the Dittaino fault system; see the schematic representation in Figure 2d). Locally, post-early-Pliocene 30° clockwise vertical axis rotations of the thrust-ridges have been related to the activity of the wrench zone [*Monaco and De Guidi*, 2006] that appears to also control the course of the major river flowing in the area (the Dittaino River; Figure 2d).

Overall, fault propagation produced a significant topographic imprint in the landscape. An analysis of a 90×90m cell-size resolution digital terrain model (DTM) (SRTM30, http://www2.jpl.nasa.gov/srtm) revealed the occurrence of a NW-SE trending topographic high in the SW side of the wrench zone (Figure 3d). Along-strike and transversal elevation profiles confirm topography perturbations in the vicinity of the fault zone. The most prominent topographic anomaly occurs in the Madonie Mountains that, in contrast with the average elevation of the entire SCZ and CA (~500 m asl), have reached the topographic elevation of about 2000 m asl (profile A-A′). This topographic anomaly continues toward SE becoming less pronounced in the central part of the boundary (profile B-B′). Along the belt direction, topography gently decreases from NW to SE (profile C-C′), in line with the fault propagation.

3.3. Gravimetric Data

Bouguer gravity anomalies available for the studied region ("Digital Gravity Maps of Italy at 1: 250.000 scale," http://www.isprambiente.gov.it/en/projects/soil-and-territory/Digital-Gravity-Maps-of-Italy) have been analyzed to obtain information on the crustal nature/density of blocks located in the two sides of the wrench zone (Figure 4). Regional gravimetric profiles passing through the boundary show that Bouguer anomalies gently decrease from NE to SW (Figure 4, right) even if this trend is perturbed by relative maxima occurring roughly along the wrench zone (e.g., profiles A-A′ and B-B′). To better investigate buried tectonic boundaries, we used a recently published gravimetric gradient map of the central Mediterranean [*Barreca*, 2014b], in which the major tectonic lineaments/paleo-margins can be imaged by lateral density contrast (colored map in the background of Figure 4). We noted that the N170E trending steep gradient signal (red in Figure 4), produced by the Mesozoic ocean-continent transition along the Malta Escarpment, assumes a NW-SE direction (N135E) south of Mount Etna. Toward the NW, the NW-SE oriented gravimetric lateral contrast becomes less evident. This is probably due to the superposition in this sector of the Sicilian chain above the buried paleo-margin. Despite that, the lateral contrast can be more or less followed all over the central-eastern Sicily as far as the town of Cefalù in the Tyrrhenian coastal domain.

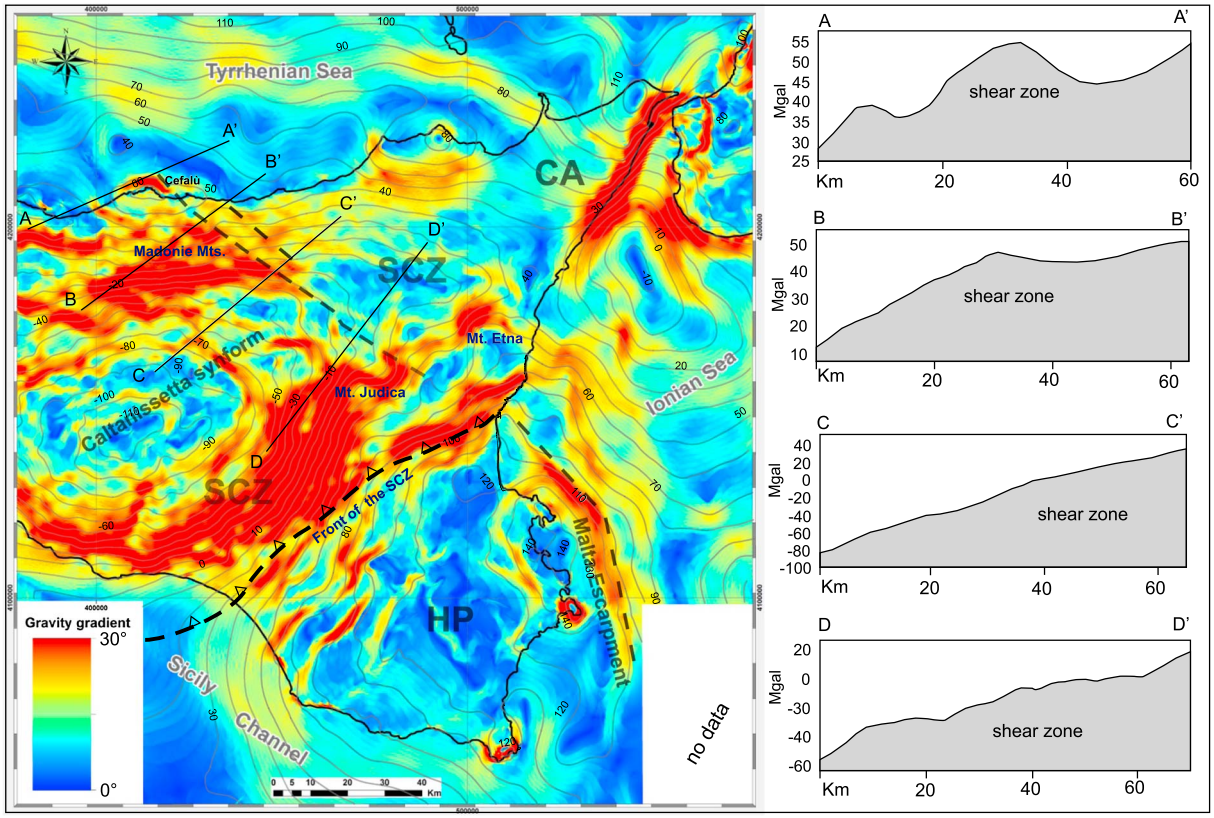

Figure 4. Combined view of Bouguer anomalies contours (mgal) and gravimetric gradient map (in the background) of central-eastern Sicily showing the lateral density variation (red gradient for the highest, blue for the lowest one) used to detect buried or near-surface geological bodies. Steepest and linear-shaped gradients are referred to tectonic boundaries or ancient margins that separate high-density rocks from soft rocks (see *Barreca* [2014b] for explanation). The NNW-SSE oriented red signal produced by the ocean-continent transition of the Malta Escarpment became NW-SE oriented. It passes south of Mount Etna and can be followed over the central eastern Sicily (black dashed lines). This gives us useful information on the spatial location of the Hyblean passive margin, the best condition for the inception of a STEP fault [see also *Baes et al.*, 2011].

The NW-SE oriented gravimetric contrast separates a zone of steep, NE-SW trending gradients (e.g., in the Madonie Mountains and Mount Judica area; Figure 4), to the SW, from a zone of low-moderate lateral contrasts, to the NE (the NE corner of Sicily). We interpret the steep gradients in the SW as the result of the Neogene-Quaternary deep-seated thrusting involving the Pelagian continental paleo-margin (see section 3) and the zone with low-moderate lateral contrasts as a thinned crustal domain not involved in deep-seated thrusting. The NW-SE trending gravimetric contrast could be related to the Mesozoic boundary between continental and thinned crusts (see tomography in section 3.3). Since it roughly matches with the field geological and topographic signature of the wrench zone, we suggest that this ancient boundary likely favored the development of the shear zone during Plio-Quaternary times.

3.4. Seismic Data

In order to define the ongoing seismotectonic processes of the area in question, we examined the regional seismic pattern. Figure 1b shows the seismicity recorded in the central Mediterranean over the 1981–2012 period as extracted from the Istituto Nazionale di Geofisica e Vulcanologia catalogues (http://csi.rm.ingv.it/; http://bollettinosismico.rm.ingv.it/index.php); it includes about 15,000 earthquakes ($1.0 < M < 5.5$) with hypocentral depth down to 40 km and up to 2000 deeper events down to 300 km located in the southern Thyrrhenian Sea (see red dots in Figure 1b) and related to the narrow subducting Ionian crust.

Assuming a clustering of events around active faults, the earthquakes distribution may reveal the most important regional lineaments and seismic zones where the higher earthquake density occurs. In particular, focusing on mainland Sicily, earthquakes clearly highlight a WNW-ESE oriented seismic trend that roughly

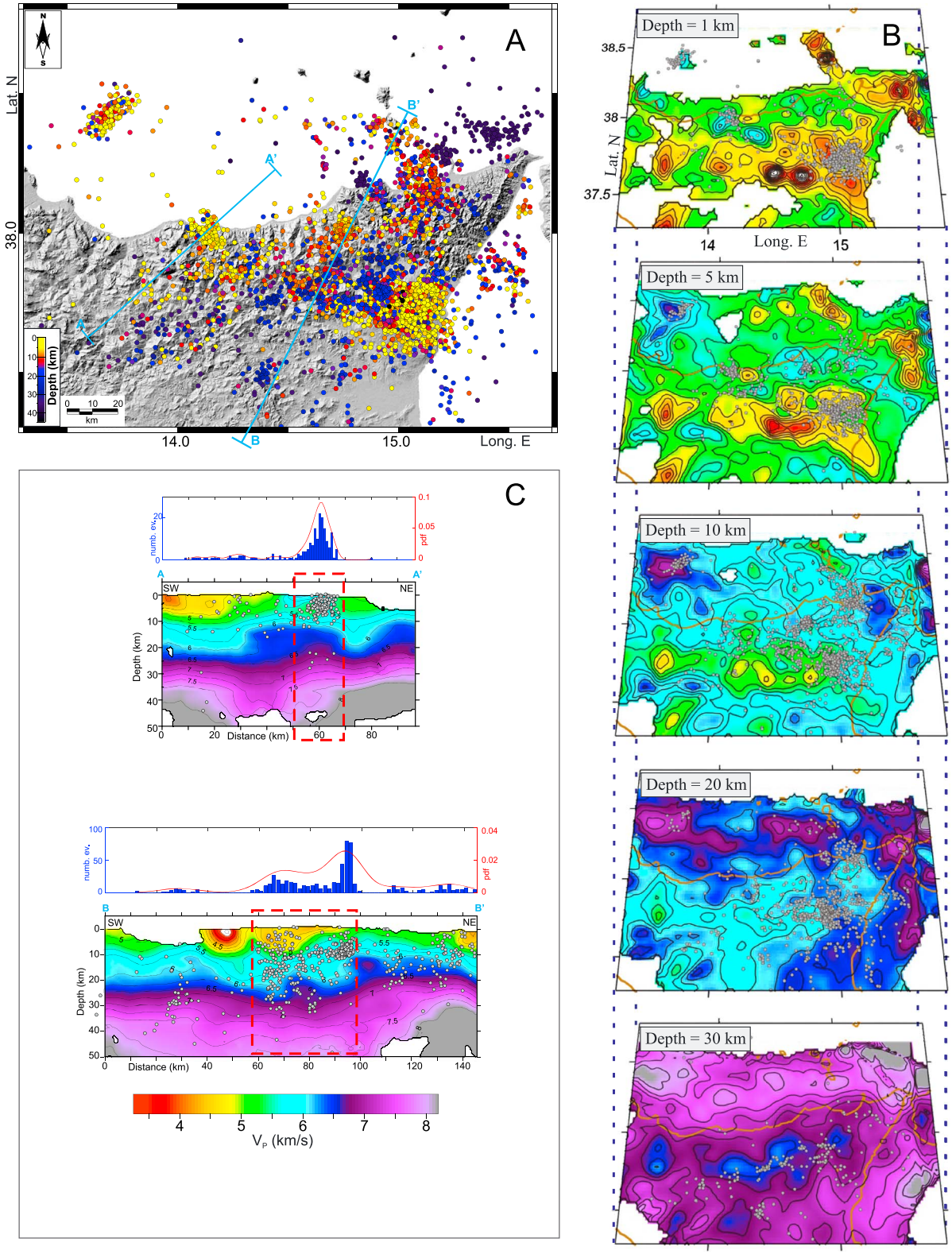

Figure 5. (a) Map view and depth distribution of the selected earthquakes, after the tomographic inversion. (b) V_P model for some representative layers resulting from the 3-D inversion. The contour lines are at intervals of 0.25 km/s. The grey circles represent relocated earthquakes within half the grid size of the slice. (c) Vertical sections through the model, showing also the relocated earthquakes within +10 km from the sections (the traces of the sections are reported in the map). The red dashed rectangles indicate the position of the hypothesized wrench zone. At the top of the vertical sections, the panels represent (i) the histogram (in blue) of the earthquake count along the considered sections and (ii) the corresponding estimated probability density function (red solid line).

matches the structural lineament described above (see sections 3.1 and 3.2) and which appears to separate a zone with very few seismic events in the SW from a zone more prone to release earthquakes in the NE.

To investigate about this seismic pattern further, we performed a seismic tomography inversion over the central-eastern Sicily. This procedure leads to significantly improve the hypocentral locations and to obtain a 3D velocity model of the region that, being closely dependent on the crustal structure, aids the seismotectonic interpretation by tracing the characteristics of a fault system. To this end, we applied the LOTOS algorithm [*Koulakov*, 2009], which uses a self-adapting grid geometry, based on the ray density, to reduce possible bias of the resulting models due to the grid configuration (e.g., overly large node spacing to suitably image the size of genuine anomalies). Specifically, in the absence of rays no node is installed, whereas in areas of higher ray density, the spacing of the grid can be kept considerably smaller up to a predetermined minimum value (in our case, 5 and 3 km for the horizontal and vertical step, respectively).

Earthquake data, in the area 13.10–15.58 long E, 37.10–38.40 lat N, were filtered according to quality criteria, i.e., by selecting events with at least 10 observations (on average 12 *P* and 6 *S* phases) and rejecting some of the arrivals with residuals of more than 1.5 s for *P* and 2 s for *S* rays; 90 percentile of azimuthal GAP is 235°. The final data set consisted of about 49,300 P and 28,500 *S* arrival times from about 4000 earthquakes ($1 < M < 5.5$), which were jointly inverted starting with the 1-D velocity model by *Sgroi et al.* [2012]. The reliability of the tomographic results was verified by testing with synthetic models in order to identify badly resolved areas in the solution. In practice, we calculated theoretical travel times of the seismic rays for some velocity test models. The synthetic data were then inverted using the same starting model and control values as for the real data. By comparing the results of these inversions with the target models (i.e., test models), we can detect unrestored zones that correspond to areas where tomographic resolution is low (see Appendix for a full illustration). The synthetic tests prove the capability of the tomography to recover 10 km sized anomalies, at least down to a depth of 30 km (see Figure A1). In addition, the inversion improved the quality of the final locations with respect to the initial guess, reducing the RMS by about 30% for *P* and *S* data, with average residuals of 0.30 s and 0.40 s, respectively.

The hypocentral distribution, resulting from the accurate events relocation, depicts the seismic pattern between the Madonie Mountain and the Mount Judica area (Figure 1c). It seems to be characterized by vertically clustered events that are found down to a depth of about 35 km (Figures 5a and 5c). The estimated earthquake density (see histograms at the top of the cross sections in Figure 5) highlights an increase in the seismic rate along the structural belt. This feature is also accompanied by a significant lateral velocity perturbation such as to the south of Mount Etna, where a sharp velocity variation occurs along a NW-SE trend, matching closely the steepest gravimetric gradient (see section 3.2). A dislocated low-velocity and shallow body in the NW (see the 5 km depth slices in Figure 5b) points to a right-lateral movement. Moreover, the images in the tomography sections seem to point to a transition between two crustal compartments with different thickness, higher (about 35 km) in the SW, lower (about 25 km) in the NE (see the velocity images in Figure 5c).

Focal mechanisms were computed for the major and best-recorded earthquakes, using the FPFIT algorithm [*Reasenberg and Oppenheimer*, 1985], which used *P* wave polarity data and their spatial distribution on the focal sphere. Polarities were extracted from the "Sicily and southern Calabria focal mechanism database" [http://sismoweb.ct.ingv.it/focal/; see *Scarfì et al.*, 2013], which reports data and focal plane solutions (FPSs) for events recorded since 2000 and with a magnitude of at least 2.7. Data were inverted together with the rays traced through the computed 3-D velocity model. After discarding solutions not matching minimum quality criteria—i.e., averaged uncertainties in strike, dip, and rake greater than 30° and multiple solutions with different faulting styles (e.g., a normal and a strike-slip fault)—we collected 132 well-constrained crustal FPSs. In addition, we included some solutions falling in the studied area published by *Neri et al.* [2005], *Sgroi et al.* [2012], and *Musumeci et al.* [2014]; this led to add 63 new FPSs, thus obtaining a larger data set in time (1991–2013) and magnitude ($1.3 < M < 5.9$). Note that we excluded the seismicity related to the complex structures of the Etna volcano from our analysis, as this was beyond the scope of the work.

Fault plane solutions (Figure 6) reveal that NE Sicily is dominated by prevailing extensional focal mechanisms with nodal planes striking mainly NE-SW and subordinately NW-SE. Conversely, there are strike-slip

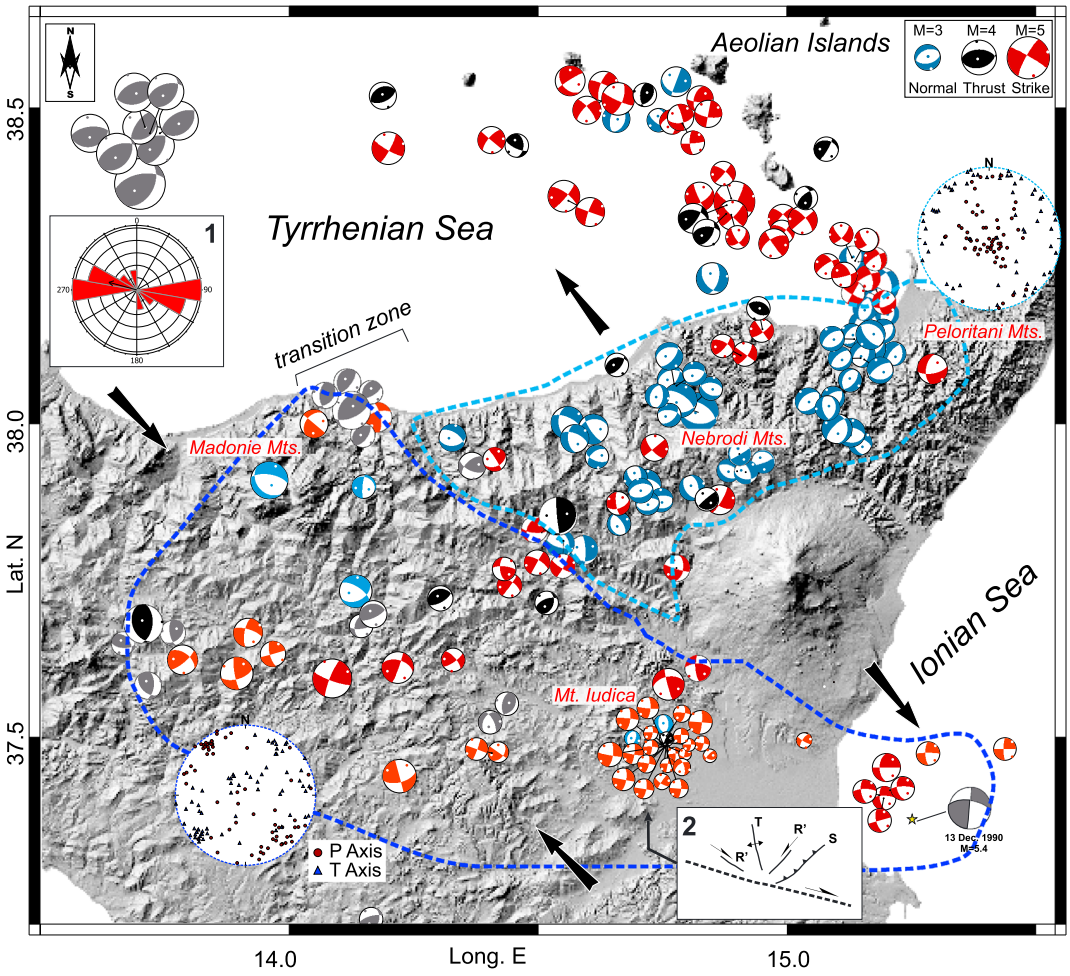

Figure 6. Map showing the selected fault plane solutions (lower hemisphere projection). Colors are red, strike-slip fault; blue, normal fault; and black, inverse fault, according to *Zoback* [1992] classification (FPSs with slightly lighter colors are from literature). Stereonets show plunges of *P* and *T* axes of the focal mechanisms into the two areas bordered by the dotted lines (see text for further details). Inset 1 shows the trend of nodal planes (selected according to field deformation) occurring within the transition zone. Inset 2 shows a kinematic model reconstructed from focal solutions.

and reverse-oblique kinematics in central Sicily, characterized by a subhorizontal NW-SE trending *P* axis (see plots in Figure 6). The analyzed boundary appears to separate these two kinematically different zones, although a number of dextral strike-slip solutions with roughly WNW-ESE trending nodal planes (see inset 1 in Figure 6) do occur alongside.

4. Data Analysis

Regional and field data compared with fault plane solutions and 3-D earthquake distribution enable obtaining a complete overview on the architecture and kinematics of the analyzed shear zone. This probably consists of a more or less developed lithospheric-scale deformation belt that, in the near-surface, is scattered into a series of discrete segments, which occasionally overlap to form zones of releasing/restraining step overs. Geostructural data collected at key sectors suggest that during Plio-Pleistocene times, nonuniform motion occurred along a right-lateral wrench zone. It can be therefore divided into three large-scale segments.

The northern segment bounds the Panormide nappe outcropping in the Madonie Mountains to the East (see also the Mount San Salvatore to Mount Alburchia fault of *Barreca et al.* [2010b]) and exhibits mostly normal-oblique deformation with large vertical (~2.7 km; see Figure 3b) and lateral (20 km; see Figure 3a) offsets.

Diffused normal faults crosscut the Pliocene thrusts along the Madonie Mountain range [*ISPRA,* 2012]. The central segment, bordering the major synclines, seems to have been characterized by prevailing right-lateral transpressional deformation, as suggested by vertical-axis rotations and fold interference pattern. The southern segments (the area between the Centuripe Basin and the Mount Judica thrust-stack/restraining step over) are characterized by right-lateral transpressional kinematics distributed over a larger band (15–20 km wide). The age of the basins involved in rotations and the decreasing magnitude of rotation from NW to SE (56° in the Gangi, 35° in the Nicosia, and 30° in the Centuripe synclines; see Figure 2E) suggests a progressive southeastward propagation of the wrench fault.

Current kinematics is depicted by focal solutions (see section 3.3), which highlight that seismic faulting along the analyzed belt predominantly occurs by strike-slip, normal, and subordinately by reverse-oblique kinematics. NW-SE trending right-lateral focal mechanisms prevail alongside the central-northern part of the shear zone, whereas they shift to WNW-ESE directions at the tip zone (e.g., Mount Judica area; see inset 1 in Figure 6). Here WNW-ESE oriented right-lateral fault solutions (roughly located alongside the Dittaino river; Figure 2a) are accompanied by events with different mechanisms probably nucleated along the NW-SE trending synthetic R, NNE-SSW striking antithetic R′, and ~N-S extensional T and NE-SW reverse-oblique S Riedel structures (see inset 2 in Figure 6). Earthquakes scattered on associated structures are all compatible with a transpressional regime (dominated by a roughly NNW-SSE oriented max stress axis) and also point to strain partitioning in an early stage of deformation along the immature tip zone.

As revealed by 3-D epicenters distribution and seismic tomography, the shear zone is at least a deep-crustal (30–40 km deep) structural discontinuity developed at the transition between distinct crustal sectors, a thicker one to the SW and a thinner one (probably transitional to the subducting Ionian domain) to the NE. This transition zone is also marked by a strong anisotropy in the seismicity pattern (see section 3.3 and the tomographic section in Figure 5c), separating a sector in the NE with the highest number of earthquakes from the one in the SW with fewer seismic events. This peculiarity would indicate that the shear zone probably has developed along a zone of preexisting rheological transition as is also evidenced by the inherited gravimetric lateral contrast (see section 3.2). Southeast of the tip (i.e., along the NW-SE trending gravimetric contrast), the occurrence of diapirs containing serpentinite rocks of Permo-Triassic age [*Manuella et al.*, 2012; *Barreca*, 2014c] strongly supports the hypothesis that the shear zone probably propagated along a portion of an ancient ocean-continent transition domain (a zone of crustal weakness), similar to that of the Malta Escarpment, currently buried below the SCZ thrust imbricates.

5. Tectonic Evolution

The ancient and present-day kinematics reconstructed by field data and by computed focal solutions allow imaging a possible tectonic evolution of the proposed lineament (Figure 7).

During the Pliocene-Early Pleistocene, the boundary mainly worked as a dextral shear zone and its propagation produced large and time-progressive clockwise vertical axis rotations of the previously settled basin structures. The right-lateral motion, together with its trending orthogonal to the hinge of the Calabrian-Ionian subduction system (see Figure 1a), makes the detected structural belt a good candidate to play the role of a first-order kinematics boundary at the SW edge of the Ionian subduction system during that time (Figure 7a). The extreme extensional down-faulting, which affected the northern segment of the wrench zone over the same period (i.e., the Madonie Mountains; see section 3.2) reinforces this hypothesis, dip-slip faulting being expected in the upper plate near the edge of the subducted slab (Figure 7a).

Late Quaternary normal faulting [*Monaco and Tortorici*, 2000] and strong uplift [*Ferranti et al.*, 2006] along NE Sicily and the current extension in the NE side of the shear zone (see *P* axis attitude in Figure 6) indicate a recent and significant geodynamic change in the area. Accordingly, elastic rebound [see also *Westaway*, 1993; *Gvirtzman and Nur*, 1999] by slab detachment [*Neri et al.*, 2009] or mantle upwelling by lateral toroidal flow [*Piromallo et al.*, 2011; *Faccenna et al.*, 2004; *Billi et al.*, 2010] could be invoked to explain this recently-settled tectonic configuration. Slab detachment, occurred parallel to the subduction-hinge, implies the cessation of subduction and, as a result, the likely stopping of wrenching at slab edge. On the contrary, horizontal GPS velocity field [*Palano et al.*, 2012; *Devoti et al.*, 2011; *Mastrolembo Ventura et al.*, 2014] (see Figure 1a) and some NW-SE trending extensional mechanisms (see the NW-SE oriented

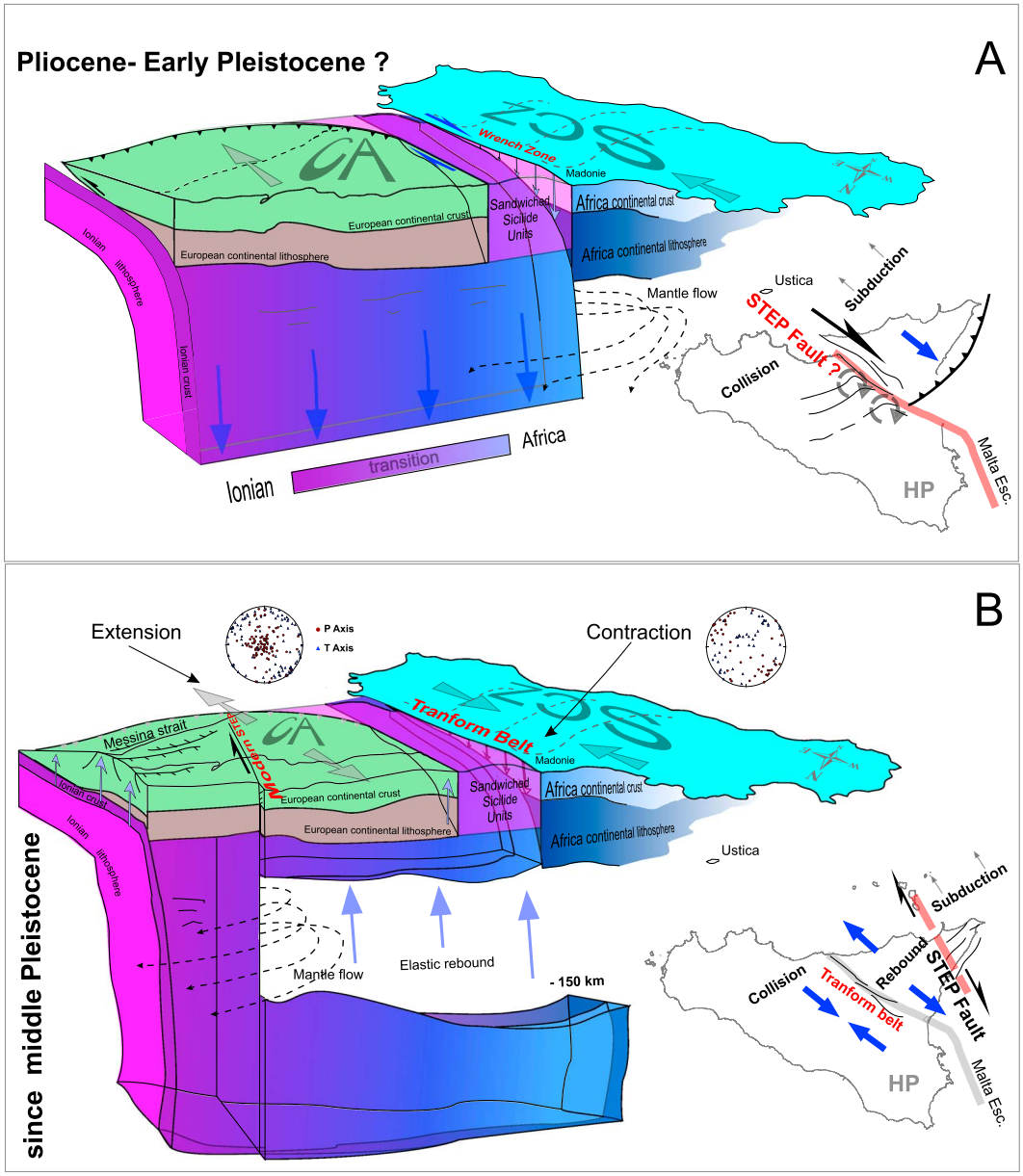

Figure 7. Reconstructed 3-D model of the Ionian/Calabrian subduction system at different stages. (a) Configuration of the subduction system as imaged during the Plio-Pleistocene ? (the inferred age for the wrench zone as it mainly involves early Pliocene sediments) when it still exhibited a continuous slab and wrench zone worked as a STEP fault producing structural rotations, progressive wrenching and kilometre-scale topography. We do not exclude mantle flow component to explain wrenching in the area [see *Faccenna et al.*, 2011]. (b) Since middle-late Pleistocene (probably), slab detachment occurred beneath eastern Sicily [see *Gvirtzman and Nur*, 1999; *Neri et al.*, 2009] causing subduction cessation and elastic rebound in the NE corner of Sicily. Elastic rebound process is corroborated by the current extension the NE side of the wrench zone (see *P* axis attitude). Taking into account that contraction still occurs (see *P* axes attitude for this sector) in the SW of the SCZ, the wrench zone could currently play the role of a transfer boundary separating the two sectors with distinct kinematics, imitating in this way the kinematics behavior of a transform fault.

fault plane solutions in Figure 6), just NE of the boundary, indicate an extensional component of deformation in the vicinity of the shear zone. Reactivation is currently testified by the development of a large seismic belt, the Cefalù-Etna seismic zone of *Billi et al.* [2010], roughly matching the orientation of the proposed structural boundary.

The seismic belt has been variously interpreted by previous researchers (i) as an incipient extension ensuing from upper crustal stretching above an active thrust belt [*Lavecchia et al.*, 2007] or (ii) as the reactivation of preexisting faults parallel to the regional maximum compression and upwelling of melt mantle material [*Billi et al.*, 2010]. Conversely, our data revealed that the analyzed boundary is currently working as a transform belt since it accommodates different kinematics in the overriding plate, extension in the NE (dominated by a subvertical *P* axis and extension axis along the E-W direction) and contraction in the SW (controlled by a subhorizontal, NNW trending *P* axis) (Figure 7b). However, a similar tectonic complexity could also be caused by toroidal mantle flow dynamics at the edge of the retreating slab [e.g., *Gvirtzman and Nur*, 1999; *Faccenna et al.*, 2004; *Funiciello et al*., 2006] (Figure 7). Strike-slip deformation, driven by the horizontal component of mantle motion, is also expected at surface [*Faccenna et al*., 2011].

6. Conclusions

The analysis of geological features and gravimetric/seismological data provides evidence for a regionally extended (about 100 km long) structural discontinuity slicing through the entire central-eastern portion of the Sicilian Collision Zone, between the Madonie Mountain range and the Mount Judica area, SW of Mount Etna volcano. The associated deformation (e.g., wrenching and time-progressive structural rotations; see Figure 3b), a substantial topographic imprint in the landscape (see Figure 3d), its location (laterally to the subducting Ionian crust; Figure 1a), and trending (orthogonal to the hinge of the subduction system) support the hypothesis that during the Pliocene-early Pleistocene (probably), the analyzed boundary served as a STEP fault (Subduction Transform Edge Propagator; in the sense of *Govers and Wortel* [2005]) or tearing zone accommodating upper plate deformation along the ancient SW edge of the Ionian Slab.

Complete slab detachment beneath NE Sicily [*Neri et al.*, 2009] produced a twofold consequence in the kinematics of the proposed boundary: (i) deactivation of the supposed STEP mechanism as a result of subduction cessation in the area and (ii) reactivation as a transform belt currently separating a recently settled zone (the NE side of the boundary) where part of the deformation is accommodated by extension from a long-standing converging sector, the rest of the Sicily island.

We conclude that the analyzed shear zone could represent the shallow expression of an incipient transform belt, separating compartments characterized by different motion in the modern context of Africa-Europe convergence and fragmentation. It has probably reactivated a former (Plio-Pleistocene?) STEP segment (never reported in literature for the continental Sicily), active before slab detachment within a larger belt within a wide crustal transition zone (Hyblean to Ionian) occurring beneath the NE corner of Sicily. According to several authors [see *Wortel et al.*, 2009; *Polonia et al.*, 2011, 2012; *Gallais et al.*, 2013; *Gutscher et al*., 2015; *Polonia et al.*, 2016; *Scarfì et al.*, 2016], modern STEP faults have developed, following retreating and narrowing of the slab breaking, along other zones of the Calabrian-Ionian subduction system.

Appendix: Tomography Reliability Analysis

Following *Koulakov* [2009], numerical experiments with synthetic models were carried out to assess the spatial resolutions provided by the data and to evaluate the optimal values of the other parameters (e.g., amplitude damping and smoothing) used for the simultaneous inversion of the 3-D velocity structure and the final hypocentres. Synthetic models give an immediate and straightforward idea of the inversion stability, potentially insignificant or artificial features and the sensitivity with respect to the choice of the starting model. In practice, we calculated theoretical travel times in two idealized velocity models: (i) one characterized by a regular pattern of high- and low-velocity zones with 10×10 km cells, commonly known as the checkerboard test and (ii) the other with several anomalies, differing in shape and size. The synthetic data were then inverted using the same starting model and control values as for the real data [see also *Scarfì et al.*, 2007, 2009 and *Musumeci et al.*, 2014]. By comparing the results of these inversions with the target models (i.e., test models), we have been able to reveal not restored zones corresponding to areas where tomographic resolution is low. The tests indicate the reliability of our tomography in the area in question of interest, being able to recover 10–15 km sized anomalies, at least down to a depth of 30 km (see Figure A1).

Results of the final inversion show a reduction of the residual average deviations by ~30% for *P* and *S* data, with remnant average residuals of 0.30 s and0.40 s, respectively.

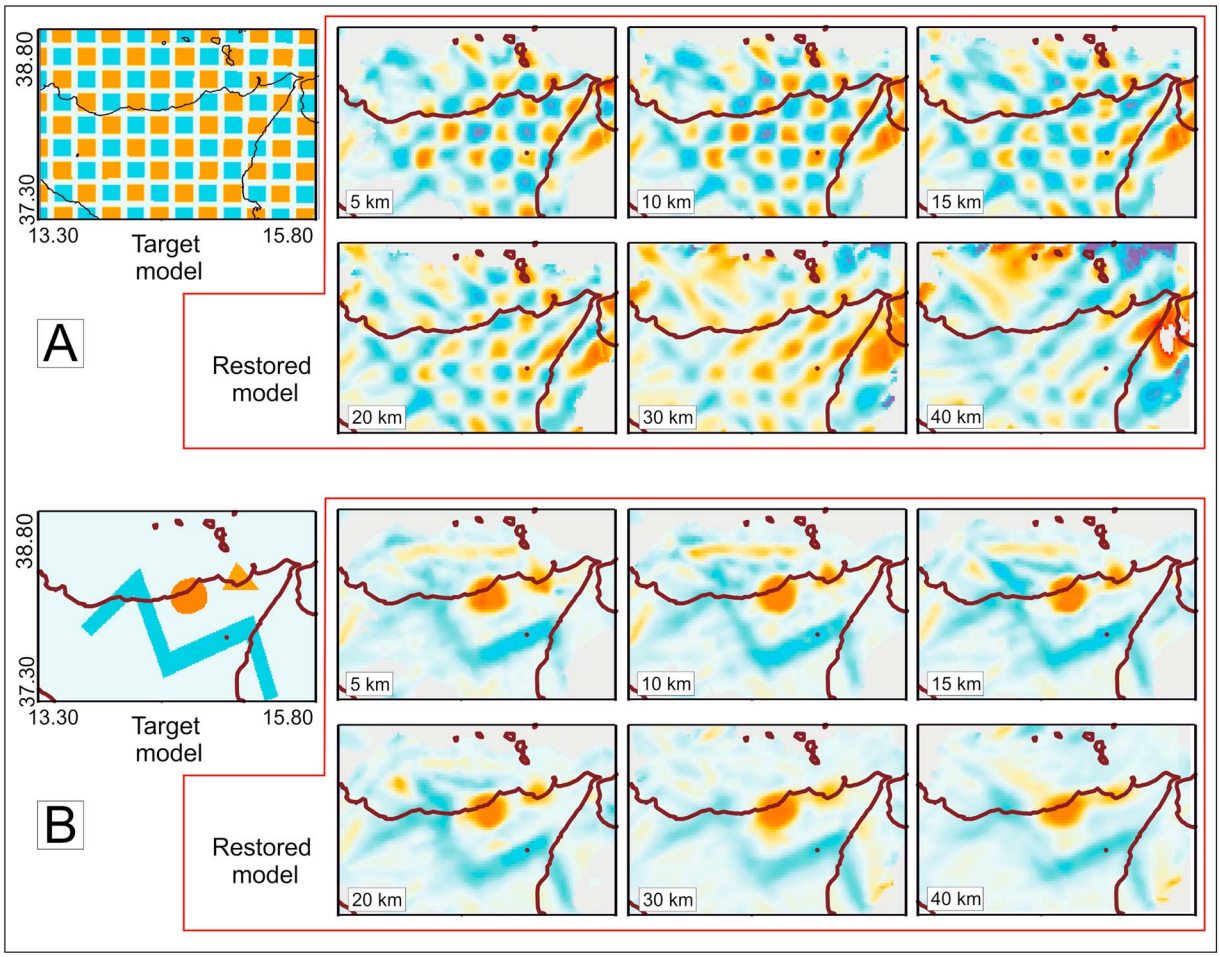

Figure A1. Wave velocity distribution obtained from the (a) checkerboard and (b) idealized resolution tests (see text for further details).

Acknowledgments
We wish to thank the Editor C. Faccenna, the Associate Editor P. Vannucchi, Z. Gvirtzman, and an anonymous reviewer for their constructive comments. This work was partially funded by PRIN 2010–11 Project "Active and recent geo-dynamics of Calabrian Arc and accretionary complex in the Ionian Sea" (responsible C. Monaco_. All the data in this paper are available by contacting the corresponding author at g.barreca@unict.it

References

Abate, B., E. Di Stefano, P. Di Stefano, C. Pecoraro, and P. Renda (1982), Segnalazione di un affioramento di "Trubi" sul massiccio di Pizzo Carbonara (Madonie, Sicilia), *Rend. Soc. Geol. Ital.*, *5*, 25–26.

Baes, M., R. Govers, and M. J. R. Wortel (2011), Subduction initiation along the inherited weakness zone at the edge of a slab: Insights from numerical models, *Geophys. J. Int.*, *184*, doi:10.1111/j.1365-246X.2010.04896.x:991-1008.

Barreca, G. (2014a), Geological-structural outlines of the southern Madonie Mts. (Central Northern Sicily), *J. Maps*, doi:10.1080/17445647.2014.977972.

Barreca, G. (2014b), Gravimetric gradient, Sicily and southern Calabria, Italy (central Mediterranean), *J. Maps*, doi:10.1080/17445647.2014.893848.

Barreca, G. (2014c), Geological and geophysical evidences for mud diapirism in south-eastern Sicily (Italy) and geodynamic implications, *J. Geodyn.*, *82*, 168–177, doi:10.1016/j.jog.2014.02.003.

Barreca, G., and F. E. Maesano (2012), Restraining stepover deformation superimposed on a previous fold-and thrust-belt: A case study from the Mt. Kumeta-Rocca Busambra ridges (western Sicily, Italy), *J. Geodyn.*, *55*, 1–17, doi:10.1016/j.jog.2011.10.007.

Barreca, G., and C. Monaco (2013), Vertical-axis rotation in the Sicilian fold and thrust belt: New structural constrains from the Madonie Mts. (Sicily, Italy), *It. J. Geosci. (Boll. Soc. Geol. Ital.)*, *132*(2), 407–421, doi:10.3301/IJG.2012.44.

Barreca, G., F. E. Maesano, and S. Carbone (2010a), Tectonic evolution of the Northern Sicanian-Southern Palermo Mountains range in Western Sicily: Insight on the exhumation of the thrust-involved foreland domains, *Ital. J. Geosci.*, *129*(3), 234–247.

Barreca, G., M. S. Barbano, S. Carbone, and C. Monaco (2010b), Archaeological evidence for Roman-age faulting in central-northern Sicily: Possible effects of coseismic deformation, in *Ancient Earthquakes*, *Geol. Soc. Am. Spec. Publ.*, *471*, 223–232, doi:10.1130/2010.2471(18).

Barreca, G., V. Bruno, C. Cocorullo, F. Cultrera, L. Ferranti, F. Guglielmino, L. Guzzetta, M. Mattia, C. Monaco, and F. Pepe (2014a), Geodetic and geological evidence of active tectonics in south-western Sicily (Italy), *J. Geodyn.*, *82*, 138–149, doi:10.1016/j.jog.2014.03.004.

Barreca, G., V. Bruno, F. Cultrera, M. Mattia, C. Monaco, and L. Scarfì (2014b), New insights in the geodynamics of the Lipari–Vulcano area (Aeolian Archipelago, southern Italy) from geological, geodetic and seismological data, *J. Geodyn.*, *82*, 150–167, doi:10.1016/j.jog.2014.07.003.

Bello, M., A. Franchino, and S. Merlini (2000), Structural model of Eastern Sicily, *Mem. Soc. Geol. Ital.*, *55*, 61–70.

Ben-Avraham, Z., and M. Grasso (1991), Crustal structure variations and transcurrent faulting at the eastern and western margins of the eastern Mediterranean, *Tectonophysics*, *75*, 269–277.
Ben Avraham, Z., M. Boccaletti, G. Cello, M. Grasso, F. Lentini, L. Torelli, and L. Tortorici (1990), Principali domini strutturali originatisi dalla collisione neogenico-quaternaria nel Mediterraneo centrale, *Mem. Soc. Geol. Ital.*, *45*, 453–462.
Bianchi, F., S. Carbone, M. Grasso, G. Invernizzi, F. Lentini, G. Longaretti, S. Merlini, and F. Moscardini (1987), Sicilia orientale: Profilo geologico Nebrodi-Iblei, *Mem. Soc. Geol. Ital.*, *38*, 429–458.
Billi, A., G. Barberi, C. Faccenna, G. Neri, F. Pepe, and A. Sulli (2006), Tectonics and seismicity of the Tindari Fault System, southern Italy: Crustal deformations at the transition between ongoing contractional and extensional domains located above the edge of a subducting slab, *Tectonics*, *25*, TC2006, doi:10.1029/2004TC001763.
Billi, A., D. Presti, B. Orecchio, C. Faccenna, and G. Neri (2010), Incipient extension along the active convergent margin of Nubia in Sicily, Italy: Cefalù-Etna seismic zone, *Tectonics*, *29*, TC4026, doi:10.1029/2009TC002559.
Billi, A., C. Faccenna, O. Bellier, L. Minelli, G. Neri, C. Piromallo, D. Presti, D. Scrocca, and E. Serpelloni (2011), Recent tectonic reorganization of the Nubia-Eurasia convergent boundary heading for the closure of the western Mediterranean, *Bull. Soc. Géol. Fr.*, *182*, 279–303.
Calò, M., C. Dorbath, D. Luzio, S. G. Rotolo, and G. D'Anna (2009), Local earthquake tomography in the Southern Tyrrhenian region of Italy: Geophysical and petrological inferences on the subducting lithosphere, in *Subduction Zone*, *Geodynamics*, vol. 3, edited by S. Lallemand, and F. Funiciello, pp. 86–100, Springer, Berlin, doi:10.1007/978-3-540-87974.
Casero, P., M. B. Cita, M. Croce, and A. De Micheli (1984), Tentativo di interpretazione evolutiva della Scarpata di Malta basata sui dati geologici e geofisici, *Mem. Soc. Geol. Ital.*, *27*, 233–254.
Catalano, R., C. Doglioni, and S. Merlini (2001), On the Mesozoic Ionian Basin, *Geophys. J. Int.*, *144*(2001), 49–64.
D'Agostino, N., E. D'Anastasio, A. Gersavi, I. Guerra, M. R. Nedimović, L. Seeber, and M. S. Steckler (2011), Forearc extension and slow rollback of the Calabrian Arc from GPS measurements, *Geophys. Res. Lett.*, *38*, L17304, doi:10.1029/2011GL048270.
Devoti, R., A. Esposito, G. Pietrantonio, A. Pisani, and F. Riguzzi (2011), Evidence of large scale deformation patterns from GPS data in the Italian subduction boundary, *Earth Planet. Sci. Lett.*, *311*, 230–241, doi:10.1016/j.epsl.2011.09.034.
Dewey, J. F., M. L. Helman, E. Turco, D. H. W. Hutton, and S. D. Knott (1989), Kinematics of the westwern Mediterranean, in *Alpine Tectonics*, edited by M. P. Coward, D. Dietrich, and R. G. Park, *Geol. Soc. London Spec. Publ.*, *45*, 265–283.
Fabbri, A., S. Rossi, R. Sartori, and A. Barone (1982), Evoluzione neogenica dei margini marini dell'Arco Calabro-Peloritano: Implicazioni geodinamiche, *Mem. Soc. Geol. Ital.*, *24*, 357–366.
Faccenna, C., T. W. Becker, F. Lucente, L. Jolivet, and F. Rossetti (2001), History of subduction and back-arc extension in the central Mediterranean, *Geophys. J. Int.*, *145*, 809–820, doi:10.1046/j.0956-540x.2001.01435.x.
Faccenna, C., C. Piromallo, A. Crespo-Blanc, L. Jolivet, and F. Rossetti (2004), Lateral slab deformation and the origin of western Mediterranean arcs, *Tectonics*, *23*, TC1012, doi:10.1029/2002TC001488.
Faccenna, C., P. Molin, B. Orecchio, V. Olivetti, O. Bellier, F. Funiciello, L. Minelli, C. Piromallo, and A. Billi (2011), Topography of the Calabria subduction zone (southern Italy): Clues for the origin of Mt. Etna, *Tectonics*, *30*, TC1003, doi:10.1029/2010TC002694.
Ferranti, L., et al. (2006), Markers of the last interglacial sea-level high stand along the coast of Italy: Tectonic implications, *Quaternary. Int.*, *145–146*, 30–54.
Finetti, I., F. Lentini, S. Carbone, S. Catalano, and A. Del Ben (1996), Il Sistema Appennino Meridionale-Arco Calabro-Sicilia nel Mediterraneo Centrale: Studio geologico-geofisico, *Mem. Soc. Geol. Ital.*, *115*, 529–559.
Finetti, I. R., F. Lentini, S. Carbone, A. Del Ben, A. Di Stefano, E. Forlin, P. Guarnieri, M. Pipan, and A. Prizzon (2005), Geological outline of Sicily and Lithospheric Tectono-dynamics of its Tyrrhenian Margin from new CROP seismic data, in *CROP PROJECT: Deep Seismic Exploration of the Central Mediterranean and Italy*, edited by I. R. Finetti, Elsevier, Amsterdam.
Frepoli, A., G. Selvaggi, C. Chiarabba, and A. Amato (1996), State of stress in the Southern Tyrrhenian subduction zone from fault-plane solutions, *Geophys. J. Int.*, *125*, 879–891.
Funiciello, F., M. Moroni, C. Piromallo, C. Faccenna, C. Cenedese, and H. A. Bui (2006), Mapping mantle flow during retreating subduction: Laboratory models analyzed by feature tracking, *J. Geophys. Res.*, *111*, B03402, doi:10.1029/2005JB003792.
Gallais, F., D. Graindorge, M.-A. Gutscher, and D. Klaeschen (2013), Propagation of a lithospheric tear fault (STEP) through the western boundary of the Calabrian accretionary wedge offshore eastern Sicily (southern Italy), *Tectonophysics*, *602*, 141–152, doi:10.1016/j.tecto.2012.12.026.
Ghisetti, F., and L. Vezzani (1982), Different styles of deformation in the Calabrian Arc [southern Italy]: Implications for a seismotectonic zoning, *Tectonophysics*, *85*, 149–165.
Goes, S., D. Giardini, S. Jenny, C. Hollenstein, H.-G. Kahle, and A. Geiger (2004), A recent reorganization in the south-central Mediterranean, *Earth Planet. Sci. Lett.*, *226*, 335–345, doi:10.1016/j.epsl.2004.07.038.
Govers, R., and M. J. R. Wortel (2005), Lithosphere tearing at STEP faults: Reponse to edges of subduction zones, *Earth Planet. Sci. Lett.*, *236*, 505–523.
Grasso, M., and W. H. Butler (1991), Tectonic controls on the deposition of late tortonian sediments in the Caltanissetta Basins of central Sicily, *Mem. Soc. Geol. Ital.*, *47*, 313–324.
Grasso, M., F. Lentini, and L. Vezzani (1978), Lineamenti stratigrafico-strutturali delle Madonie (Sicilia centro-settentrionale), *Geol. Romana*, *17*, 45–69.
Guidoboni, E., A. Muggia, C. Marconi, and E. Boschi (2002), A case study in archaeoseismology. The collapses of the Selinunte Temples (Southwestern Sicily): Two earthquakes identified, *Bull. Seismol. Soc. Am.*, *92*, 2961–2982.
Gutscher, M.-A., S. Dominguez, B. Mercier de Lepinay, L. Pinheiro, N. Babonneau, A. Cattaneo, Y. Le Faou, G. Barreca, A. Micallef, and M. Rovere (2015), Tectonic expression of an active slab-tear from high-resolution seismic and bathymetric data offshore Sicily (Ionian Sea), *Tectonics*, *34*, 39–54, doi:10.1002/2015TC003898.
Gvirtzman, Z., and A. Nur (1999), Plate detachment, asthenosphere upwelling, and topography across subduction zones, *Geology*, *27*(6), 563–566.
ISPRA – Servizio Geologico d'Italia (2012), Note illustrative della Carta Geologica d'Italia alla scala 1:50.000; Foglio 597–610 Cefalù – Castelbuono e carta geologica allegata.
Jolivet, L., and C. Faccenna (2000), Mediterranean extension and the African-Eurasian collision, *Tectonics*, *19*, 1095–1106, doi:10.1029/2000TC900018.
Kastens, K., et al. (1988), ODP Leg 107 in the Tyrrhenian Sea: Insights into passive margin and back-arc basin evolution, *Bull. Geol. Soc. Am.*, *100*, 1140–1156.
Koulakov, I. (2009), LOTOS code for local earthquake tomographic inversion. Benchmarks for testing tomographic algorithms, *Bull. Seismol. Soc. Am.*, *99*(1), 194–214, doi:10.1785/0120080013.

Lavecchia, G., F. Ferrarini, R. de Nardis, F. Visini, and S. Barbano (2007), Active thrusting as a possible seismogenic source in Sicily (Southern Italy): Some insights from integrated structural-kinematic and seismological data, *Tectonophysics*, *445*, 145–167.
Malinverno, A., and W. B. F. Ryan (1986), Extension in the Tyrrhenian Sea and shortening in the Apennines as result of arc migration driven by slab sinking in the lithosphere, *Tectonics*, *5*, 227–245, doi:10.1029/TC005i002p00227.
Manuella, F. C., S. Carbone, and G. Barreca (2012), Origin of saponite-rich clays in a fossil serpentinite-hosted hydrothermal system in the crustal basement of the Hyblean Plateau (Sicily, Italy), *Clays Clay Miner.*, *60*, 18–31.
Mastrolembo Ventura, B., E. Serpelloni, A. Argnani, A. Bonforte, R. Bürgmanne, M. Anzidei, P. Baldi, and G. Puglisi (2014), Fast geodetic strain-rates in eastern Sicily (southern Italy): New insights into block tectonics and seismic potential in the area of the great 1693 earthquake, *Earth Planet. Sci. Lett.*, *404*, 77–88.
Monaco, C., and G. De Guidi (2006), Structural evidence for Neogene rotations in the eastern Sicilian fold and thrust belt, *J. Struct. Geol.*, *28*, 561–574.
Monaco, C., and L. Tortorici (2000), Active faulting in the Calabrian arc and eastern Sicily, *J. Geodyn.*, *29*, 407–424, doi:10.1016/S0264-3707(99)00052-6.
Monaco, C., S. Mazzoli, and L. Tortorici (1996), Active thrust tectonics in western Sicily [southern Italy]: The 1968 Belice earthquakes sequence, *Terra Nova*, *8*, 372–381.
Musumeci, C., L. Scarfì, M. Palano, and D. Patanè (2014), Foreland segmentation along an active convergent margin: New constraints in southeastern Sicily (Italy) from seismic and geodetic observations, *Tectonophysics*, doi:10.1016/j.tecto.2014.05.017.
Neri, G., G. Barberi, G. Oliva, and B. Orecchio (2005), Spatial variations of seismogenic stress orientations in Sicily, south Italy, *Phys. Earth Planet. Int.*, *148*, 175–191.
Neri, G., B. Orecchio, C. Totaro, G. Falcone, and D. Presti (2009), Subduction beneath southern Italy close the ending: Results from seismic tomography, *Seismol. Res. Lett.*, *80*, 63–70.
Orecchio, B., D. Presti, C. Totaro, and G. Neri (2014), What earthquakes say concerning residual subduction and STEP dynamics in the Calabrian Arc region, south Italy, *Geophys. J. Int.*, *199*, 1929–1942.
Palano, M., L. Ferranti, C. Monaco, M. Mattia, M. Aloisi, V. Bruno, F. Cannavò, and G. Siligato (2012), GPS velocity and strain fields in Sicily and southern Calabria, Italy: Updated geodetic constraints on tectonic block interaction in the central Mediterranean, *J. Geophys. Res.*, *117*, B07401, doi:10.1029/2012JB009254.
Patacca, E., and P. Scandone (1989), Post Tortonian mountain building in the Apennines: The role of the passive sinking of a relict lithospheric slab, in *The Lithosphere in Italy*, vol. 80, edited by A. Boriani et al., pp. 157–176, Atti Conv. Lincei, Rome.
Piromallo, C., T. W. Becker, F. Funiciello, and C. Faccenna (2011), Three-dimensional instantaneous mantle flow induced by subduction, *Geophys. Res. Lett.*, *33*, L08304, doi:10.1029/2005GL025390.
Polonia, A., L. Torelli, P. Mussoni, L. Gasperini, A. Artoni, and D. Klaeschen (2011), The Calabrian arc subduction complex in the Ionian Sea: Regional architecture, active deformation and seismic hazard, *Tectonics*, *30*, TC5018, doi:10.1029/2010TC002821.
Polonia, A., L. Torelli, L. Gasperini, and P. Mussoni (2012), Active faults and historical earthquakes in the Messina Straits area (Ionian Sea), *Nat. Hazard. Earth Syst. Sci.*, *12*, 2311–2328, doi:10.5194/nhess-12-2311-2012.
Polonia, A., et al. (2016), The Ionian and Alfeo-Etna fault zones: New segments of an evolving plate boundary in the central Mediterranean sea?, *Tectonophysics*, doi:10.1016/j.tecto.2016.03.016.
Pondrelli, S., C. Piromallo, and E. Serpelloni (2004), Convergence vs. retreat in Southern Tyrrhenian Sea: Insights from kinematics, *Geophys. Res. Lett.*, *31*, L06611, doi:10.1029/2003GL019223.
Pondrelli, S., S. Salimbeni, G. Ekström, A. Morelli, P. Gasperini, and G. Vannucci (2006), The Italian CMT dataset from 1977 to the present, *Phys. Earth Planet. Inter.*, *159*(3–4), 286–303, doi:10.1016/j.pepi.2006.07.008.
Presti, D., A. Billi, B. Orecchio, C. Totaro, C. Faccenna, and G. Neri (2013), Earthquake focal mechanisms, seismogenic stress, and seismotectonics of the Calabrian Arc, Italy, *Tectonophysics*, *602*, 153–175.
Reasenberg, P. A., and D. Oppenheimer (1985), Fortran computer programs for calculating and displaying earthquake fault-plane solutions, *U.S. Geol. Surv., Open File Rep. 85–379*.
Roure, F., D. G. Howell, C. Muller, and I. Moretti (1990), Late Cenozoic subduction complex of Sicily, *J. Struct. Geol.*, *12*, 259–266.
Sartori, R. (2003), The Tyrrhenian back-arc basin and subduction of the Ionian lithosphere, *Episodes*, *26*(3), 217–221.
Scandone, P. (1979), Origin of the Tyrrhenian Sea and Calabrian Arc, *Boll. Soc. Geol. Ital.*, *98*, 27–34.
Scarfì, L., E. Giampiccolo, C. Musumeci, D. Patanè, and H. Zhang (2007), New insights on 3D crustal structure in southeastern Sicily (Italy) and tectonic implications from an adaptive mesh seismic tomography, *Phys. Earth Planet. Inter.*, *161*, 74–85.
Scarfì, L., H. Langer, and A. Scaltrito (2009), Seismicity, seismotectonics and crustal velocity structure of the Messina Strait (Italy), *Phys. Earth Planet. Inter.*, *177*, 65–78, doi:10.1016/j.pepi.2009.07.010.
Scarfì, L., A. Messina, and C. Cassisi (2013), Sicily and Southern Calabria focal mechanism database: A valuable tool for the local and regional stress field determination, *Ann. Geophys.*, *56*(1), D0109, doi:10.4401/ag-6109.
Scarfì, L., G. Barberi, C. Musumeci, and D. Patanè (2016), Seismotectonics of Northeastern Sicily and Southern Calabria (Italy): New constraints on the tectonic structures featuring in a crucial sector for the Central Mediterranean geodynamics, *Tectonics*, *35*, 812–832, doi:10.1002/2015TC004022.
Schellart, W. P., J. Freeman, D. R. Stegman, L. Moresi, and D. May (2007), Evolution and diversity of subduction zones controlled by slab width, *Nature*, *446*, doi:10.1038/nature05615.
Şengör, A. M. C. (1979), Mid-Mesozoic closure of Permo-Triassic Tethys and its implications, *Nature*, *279*, 590–593, doi:10.1038/279590a0.
Sgroi, T., R. De Nardis, and G. Lavecchia (2012), Crustal structure and seismotectonics of central Sicily (southern Italy): New constraints from instrumental seismicity, *Geophys. J. Int.*, *189*, 1237–1252.
Vai, G. B. (2003), Development of the palaeogeography of Pangaea from Late Carboniferous to Early Permian, *Palaeogeogr. Palaeoclimatol. Palaeoecol.*, *196*, 125–155.
Westaway, R. (1993), Quaternary uplift of southern Italy, *J. Geophys. Res.*, *98*, 21,741–21,772, doi:10.1029/93JB01566.
Wortel, R., and W. Spakman (2000), Subduction and slab detachment in the Mediterranean-Carpathian region, *Science*, *290*, 1910–1917.
Wortel, R., R. Govers, and W. Spakman (2009), Continental collision and the STEP-wise evolution of convergent plate boundaries: From structure to dynamics, in *Subduction Zone Geodynamics, Subduction Zone Geodynamics Conference, Montpellier 2007*, edited by S. Lallemand and F. Funiciello, pp. 47–59, Springer, Berlin.
Zoback, M. L. (1992), First- and second-order patterns of stress in the lithosphere: The World Stress Map Project, *J. Geophys. Res.*, *97*(B8), 11,703–11,728, doi:10.1029/92JB00132.